Characterization of Ravn virus viral shedding dynamics in experimentally infected Egyptian rousette bats (*Rousettus aegypticus*)

Jessica A. Elbert,[1] Amy J. Schuh,[2,3] Brian R. Amman,[2] Jonathan C. Guito,[2] James C. Graziano,[2] Tara K. Sealy,[2] Elizabeth W. Howerth,[1] Jonathan S. Towner[1,2]

AUTHOR AFFILIATIONS   See affiliation list on p. 12.

ABSTRACT   Marburg virus (MARV) and Ravn virus (RAVV), the only two known members of the species *Orthomarburgvirus marburgense* (family *Filoviridae*), are causative agents of Marburg virus disease, a severe viral disease that typically emerges in sub-Saharan Africa and is characterized by human-to-human transmission and high case fatalities. Despite the robust characterization of MARV experimental infection in Egyptian rousette bats (ERBs; *Rousettus aegyptiacus*; common name: Egyptian rousettes), a natural MARV reservoir, experimental infection with RAVV in ERBs has not been completed. Here, we experimentally infect 12 ERBs with RAVV and quantify viral loads in blood, oral swabs, and rectal swabs over a 21-day timeline with serological and cumulative shedding data and baseline clinical parameters. Compared to previously described experimental MARV infection in ERBs, these bats experimentally inoculated with RAVV had significantly higher and prolonged rectal viral shedding loads, as well as significantly prolonged oral shedding and higher peak viremia. All ERBs seroconverted by 21 days post-infection. Additionally, all ERBs demonstrated marked heterogeneity in RAVV viral shedding loads consistent with the Pareto Principle and viral "supershedders." Our results introduce the possibility of variation in transmission dynamics and subsequent spillover differences between RAVV and MARV.

IMPORTANCE   Ravn virus, along with Marburg virus, causes severe viral disease in humans with high fatality but little to no clinical disease in its reservoir host, the Egyptian rousette bat. Our findings provide important insights into how Ravn virus behaves in its natural reservoir host, showing that Ravn virus infection followed a similar timeline to Marburg virus infection, with virus detected in blood, saliva, and feces. However, Ravn virus-infected bats had higher levels of viral shedding and shed the virus for a longer period, particularly in feces, compared to Marburg virus. These differences in viral shedding may impact the spread of the virus within bat populations and potentially alter the likelihood of spillover into humans, non-human primates, and other animal species. These insights are crucial for understanding Ravn virus maintenance in its bat reservoir and improving our ability to mitigate or prevent future human outbreaks.

KEYWORDS   Ravn virus, Marburg virus, Egyptian rousette bat, filovirus, bat

Marburg virus (MARV) and Ravn virus (RAVV), viral relatives to Ebola virus, are the only two known members of the species *Orthomarburgvirus marburgense* (family *Filoviridae*, genus *Orthomarburgvirus*) and are the causative agents of Marburg virus disease (MVD), a severe and often fatal disease that typically emerges in sub-Saharan Africa characterized by human-to-human transmission and high case fatality ratios up to 90% (1). MARV was first identified in 1967 after laboratory workers in Marburg and

Frankfurt, Germany and Belgrade (former Yugoslavia) became ill after working with African green monkeys imported from Uganda (2). To date, there have been 18 known MARV outbreaks, the most recent of which occurred in Tanzania in January 2025 (3). RAVV was first identified in 1987 following a fatal VHF case in a tourist who visited Kitum Cave in Mount Elgon National Park, Kenya (4). Designated as a distinct virus within the *Orthomarburgvirus marburgense* species in 1996, RAVV has since been identified in two subsequent outbreaks, with the most recent case reported in Uganda in 2007 (4–6). Although details about its natural distribution are limited, RAVV has only been detected in regions of Africa where Egyptian rousette bats (*Rousettus aegyptiacus,* common name: Egyptian rousettes) are found (7, 8).

The Egyptian rousette bat (ERB) is a pteropodid bat (order Chiroptera, family Pteropodidae) that inhabits parts of Africa, western Asia, the Mediterranean, and the Indian subcontinent (9). One of the few pteropodid bats capable of echolocation, they are predominantly cave-dwelling, gregarious, and social animals living in densely packed roosts (9). Numerous longitudinal ecological studies have identified the ERB as a natural reservoir host for both RAVV and MARV (6, 8, 10–13). These studies revealed that adult ERBs had the highest IgG antibody levels, while juvenile bats (approximately 6 months old) showed the highest levels of active infection, along with a temporal association between MARV disease spillover to humans and seasonal, biannual pulses of active MARV infection in juvenile ERBs (6, 10, 14). MARV and RAVV have been isolated multiple times from ERBs sampled in Uganda (6, 10, 15).

Despite being within the same viral species, the full genomic sequence of RAVV differs by up to 21% from MARV, and the amino acid sequence of the RAVV glycoprotein (GP) differs by ~22% from MARV GP (6, 16). Bayesian coalescent analysis has estimated that the most recent common ancestor (MRCA) between MARV and RAVV was approximately 700 years ago, with the known human and bat RAVV isolates sharing an MRCA approximately 50 years ago (17). A phylogenetic tree highlighting a subset of complete MARV and RAVV genomes is provided in Fig. 1.

Experimental studies have identified the ERB as a competent natural reservoir model for MARV (11, 18–21) and have also documented successful horizontal transmission of MARV between experimentally inoculated and naïve co-housed ERBs (14). ERBs experimentally inoculated with MARV have transient subclinical disease characterized by viremia (mean duration = 6.0 days, mean day of mean peak load = 6.8 DPI) (14), oral shedding (mean duration = 4.6 days, mean day of mean peak load = 9.1 DPI) with successful isolation of infectious MARV from 9/51 (17.6%) of MARV RT-qPCR-positive oral swabs (14), and rectal shedding (mean duration = 1.5 days, mean day of mean peak load = 6.8 DPI) (14). MARV shedding in the urine of experimentally infected ERBs has been documented but is limited by the challenging nature of the non-invasive specimen collection and is not fully characterized (14, 21). In previous studies, MARV-inoculated ERBs robustly seroconverted to MARV, with MARV IgG antibodies peaking between 12 and 28 DPI (14, 20, 21), followed by a decline of antibody levels falling below the threshold of seropositivity by 3 months post-infection (14). Despite diminished IgG levels, robust longstanding immunity to reinfection upon experimental challenge with MARV has been documented in ERBs up to 2 years after initial infection (22).

MARV has been well studied in numerous animal models and *in vitro* and *in vivo* experimental studies, including recent research utilizing transcriptomics, to elucidate ERB immunology and responses to infection (23–35). However, there has been limited experimental characterization of RAVV and of comparisons of virulence between RAVV and MARV. To date, the few studies utilizing RAVV include vaccine efficacy studies in cynomolgus macaques (36, 37), mice (38), and guinea pigs (39), therapeutic treatment trials of MARV and RAVV infection in non-human primates with human monoclonal antibodies (40) and small interfering RNA (41), and characterization of the lack of observable clinical disease upon experimental inoculation with RAVV in ferrets (42, 43). Genetic variation between MARV and RAVV could influence transmission dynamics, pathogenicity, and, potentially, responses to treatments or vaccines. A recent study
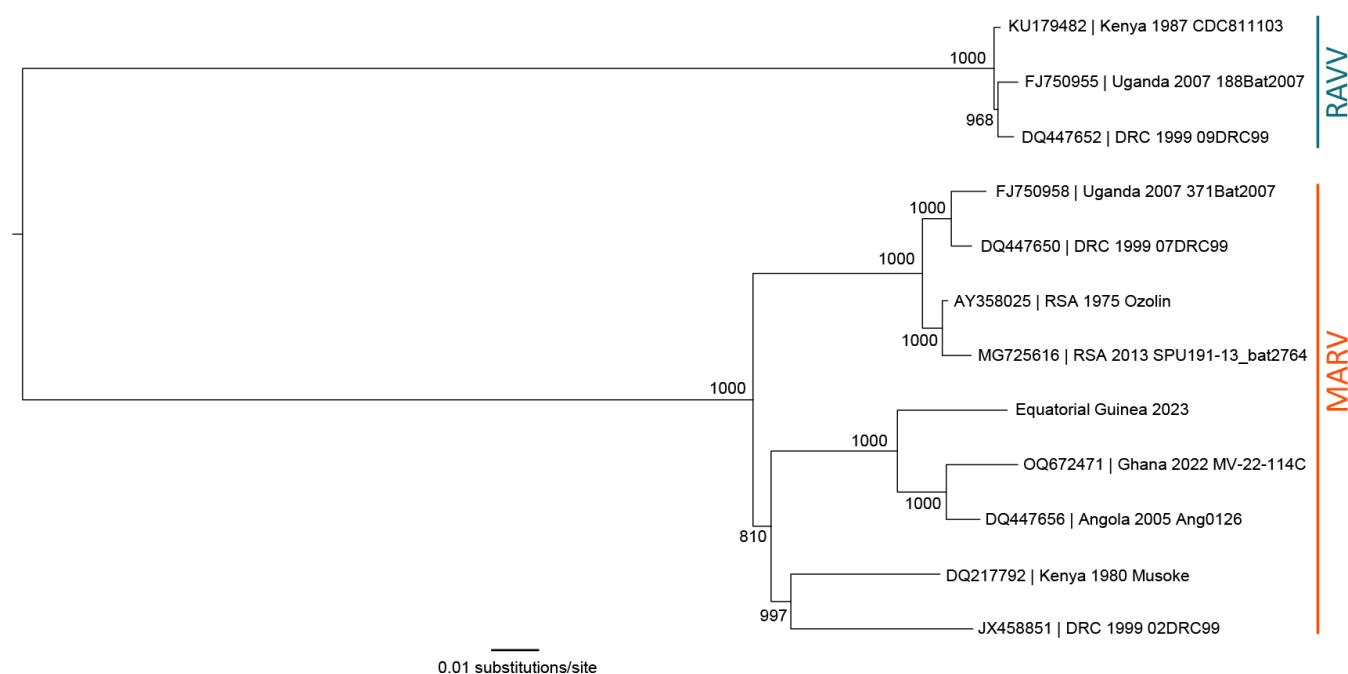
FIG 1 Midpoint-rooted, maximum-likelihood phylogeny of a subset of complete Marburg virus and Ravn virus genomes. Complete sequences from GenBank (accession numbers indicated) were aligned using Geneious Prime version 2024.0 (https://www.geneious.com/). The Equatorial Guinea 2023 sequence was acquired from https://virological.org/t/first-emergence-of-marburg-virus-in-equatorial-guinea-2023/924. ATGC Montpellier Bioinformatics Platform PhyML 3.0 (http://www.atgc-montpellier.fr/phyml/) was used to infer the maximum-likelihood tree after 1,000 bootstrap replicates. Node values indicate bootstrap support values. Scale bar indicates nucleotide substitutions per site. MARV, Marburg virus; RAVV, Ravn virus.

comparing experimental infections of different orthomarburgviruses in macaques found distinct pathogenicities between RAVV, MARV Angola, and variant isolates Musoke and Ozolin, and additionally found that despite seroconversion in all animals, RAVV is lethal in cynomolgus macaques but not rhesus macaques (44). Furthermore, a comparison of the pathogenesis of RAVV, MARV variant isolates Musoke and Popp, and MARV Angola in a serially adapted outbred guinea pig model found delayed increases in circulating inflammatory and prothrombotic elements, lower viremia levels, less severe histologic disease, and a delay in mean time to death in RAVV infection compared to MARV Angola (27). To date, experimental characterization of RAVV infection in its ERB reservoir has not been completed.

Here, we present an initial characterization of viral infection and shedding dynamics in ERBs experimentally infected with RAVV, with an aim to elucidate differences between RAVV and MARV and establish parameters for RAVV experimental infection in ERBs. We performed a 22-day experiment using 12 captive-bred and age- and sex-matched ERBs subcutaneously inoculated with a low-passage (P2) wild-type RAVV (188Bat2007) isolated from a naturally infected bat in Uganda (6). This work provides an important baseline for hypothesis-driven research, allowing a successful extrapolation of research findings in controlled laboratory settings to wild ERB populations and enabling experimental comparisons between MARV and RAVV infections. Additionally, this work furthers the continued validation of the only established reservoir model for any filovirus.

RESULTS

RAVV replication and shedding dynamics

Prior to inoculation, none of the bats had detectable viremias (Fig. 2a) or anti-RAVV IgG (Fig. 3), indicating no prior exposure to RAVV. Viral RNA levels in blood (Fig. 2a) quantified through RT-qPCR analysis of viral RNA and presented as mean $TCID_{50}$ equivalents per milliliter of fluid were consistent with previous studies that characterized MARV infection
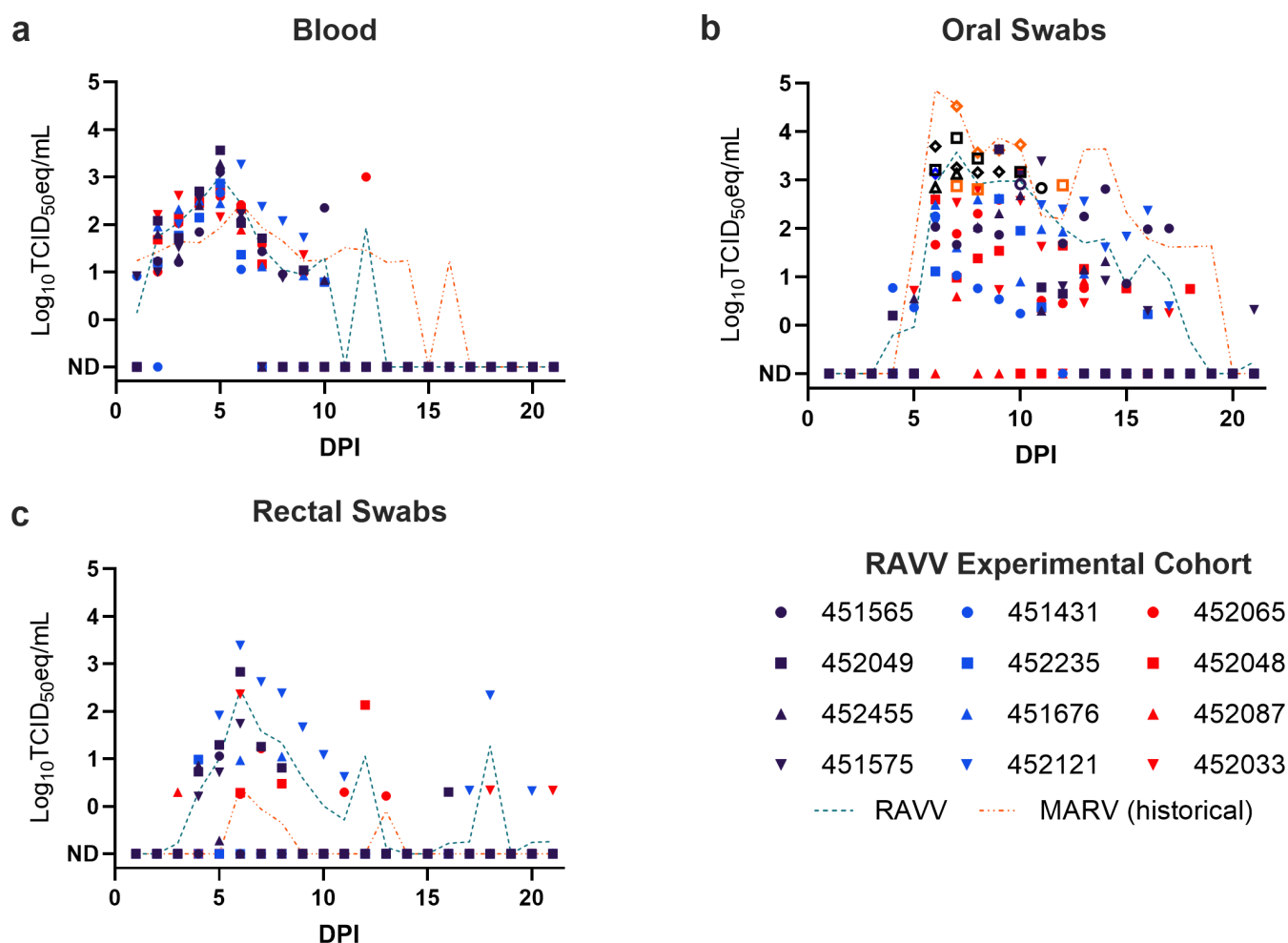
FIG 2 RAVV shedding dynamics in experimentally infected Egyptian rousette bats. RAVV loads (RT-qPCR-derived $\log_{10}$TCID$_{50}$ equivalents/mL) in (a) blood, (b) oral swabs, and (c) rectal swabs from experimentally infected Egyptian rousette bats. The teal dashed line represents the overall mean RAVV load in each sample. The orange dashed line represents the overall mean MARV load taken from historical MARV data (14). Open symbols in b represent oral swabs from which infectious RAVV was isolated. ND: not detected.

and shedding dynamics (14, 21). RAVV viremia was detected in all 12 ERBs, with mean viral load values peaking on Day 5 (mean: 1.03×10^3 TCID$_{50}$/mL; highest individual value: 3.65×10^3 TCID$_{50}$/mL) and cleared by Day 13. The highest number of viremic ERBs was on 3–6 DPI (n = 12 bats each day), with 79 positive viremic data points overall. The average length of detectable viremia was 6.6 days, ranging from 5 to 8 days. Blood samples for RT-qPCR were no longer collected after 15 DPI following three consecutive days of negative RT-qPCR results from all bats.

RAVV RT-qPCR positive oral swabs were detected in all 12 ERBs, with mean viral load values peaking on 7 DPI (mean: 3.76×10^3 TCID$_{50}$/mL; highest individual value: 3.33×10^4 TCID$_{50}$/mL) and with sporadic RT-qPCR positivity through study completion at 21 DPI. The highest number of positive oral swab specimens was 7 DPI (n = 12), with 106 positive oral swab specimens overall. The average length of oral shedding was 8.8 days, ranging from 4 to 12 days. RT-qPCR-positive oral swab specimens with CT values $\leq$ 32 were selected for virus isolation; this represented 26 out of the 106 (24.5%) RAVV RNA positive oral swab samples from eight infected ERBs (451565, n = 3 samples; 451575, n = 6; 452033, n = 2; 452049, n = 5; 452065, n = 1; 452121, n = 4; 452235, n = 3; 452455, n = 2). Infectious RAVV was isolated from 20/26 (77%) samples.
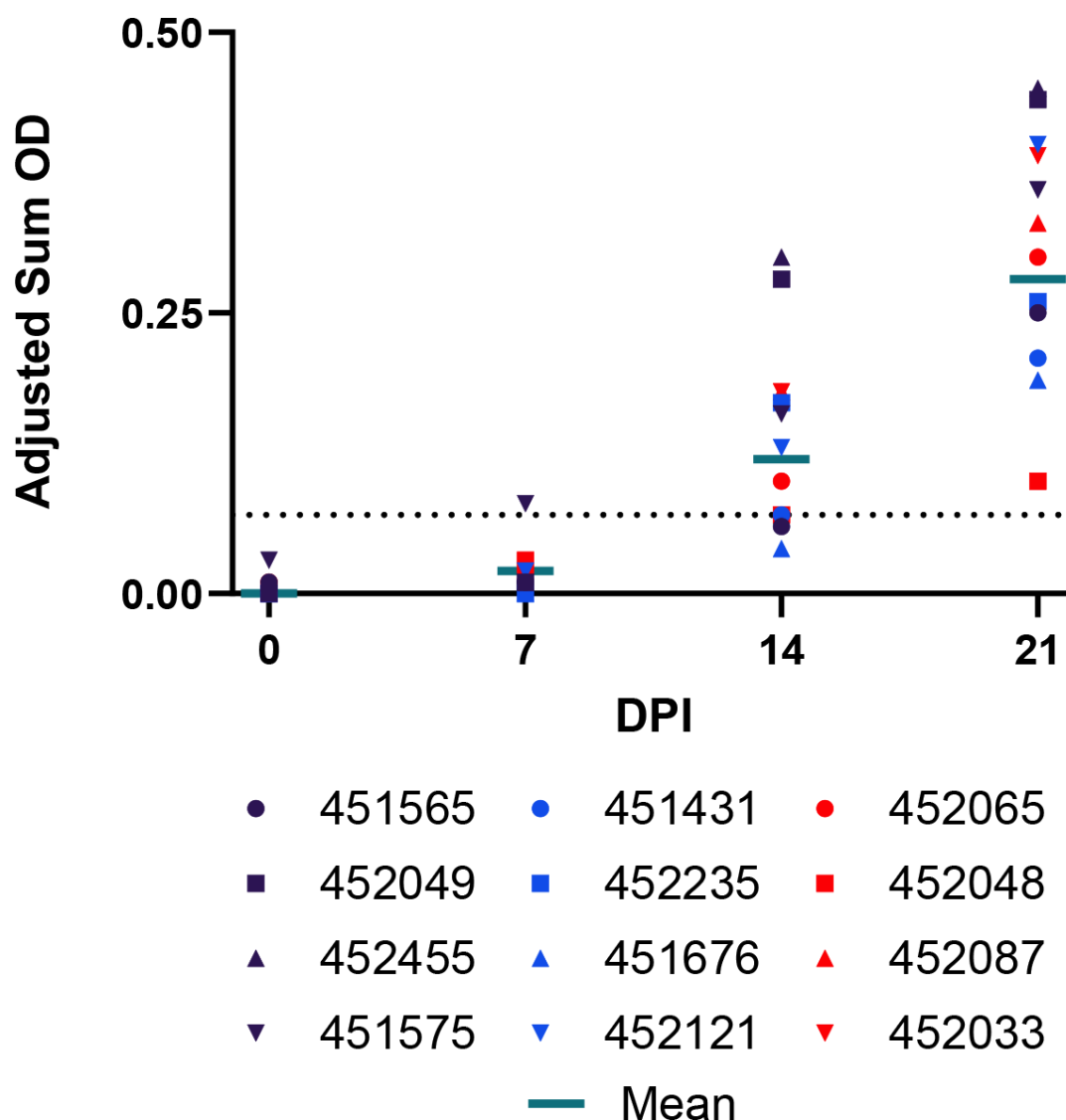
FIG 3 RAVV IgG antibody responses of experimentally infected Egyptian rousette bats. IgG antibodies were detected by ELISA with purified recombinant nucleoprotein of the Angola strain of MARV expressed in *Escherichia coli* from blood taken at 0, 7, 14, and 21 DPI. IgG antibody levels are expressed as adjusted sum OD values normalized between 0 and 1. The black dotted line represents the assay threshold (RAVV seropositive ≥ 0.07).

RAVV RT-qPCR-positive rectal swabs were detected in 11/12 (92%) ERBs, with mean viral load values peaking on 6 DPI (mean: 2.87×10^2 TCID$_{50}$/mL; highest individual value: 2.46×10^3 TCID$_{50}$/mL) and with sporadic RT-qPCR positivity through study completion at 21 DPI. Bat 451431 never had a RAVV-RT-qPCR-positive rectal swab despite having positive oral swab and blood samples. The highest number of positive rectal swab specimens was at 6 DPI ($n = 7$), with 36 positive rectal swab specimens overall. The average length of rectal shedding was 3 days, ranging from 1 to 10 days. To avoid mucosal irritation or injury, duplicate rectal swab samples were not collected for isolation; therefore, isolation attempts on rectal swab samples were not performed.

Complete seroconversion in all bats

Consistent with previous studies (14, 19–21, 45), all ERBs demonstrated a robust primary immune response, with all inoculated bats (12/12) testing RAVV seronegative at 0 DPI and subsequently seroconverting to RAVV [mean peak adjusted sum optical density (OD) = 0.28, s.d. = 0.11; Fig. 3] by 21 DPI.

Heterogeneities in oral and rectal RAVV shedding

Heterogeneity in host shedding of pathogens plays an important role in infectious disease transmission dynamics and can be measured by assessing cumulative pathogen loads shed in excretory products of naturally or experimentally infected individuals (46–57). Viral shedding was calculated for each inoculated bat by summing RAVV RNA loads detected 0–21 DPI in oral and rectal swabs. Total oral and rectal shedding varied considerably between individual bats, with sum $\log_{10}TCID_{50}$ equivalents/mL ranging from 1.21 to 4.68 (mean = 3.29, s.d. = 0.91) and undetectable to 3.54 (mean = 1.56, s.d. = 1.03), respectively. As previously demonstrated (14), the Lorenz curve and associated Gini coefficient are effective at illustrating and quantifying inequality in a distribution and herein used to highlight heterogeneity in individual RAVV oral (Fig. 4a) and rectal (Fig. 4b) shedding. For example, Fig. 4a demonstrates that 25.0% of the inoculated bats were responsible for 83.5% of RAVV oral shedding; 50.0% of the bats were responsible for 92.6% of oral shedding; and 75.0% of the bats were responsible for 99.2% of oral shedding. Figure 4b demonstrates that 25.0% of the inoculated bat population was responsible for 94.1% of RAVV rectal shedding; 50.0% of the bats were responsible for 98.9% of rectal shedding; and 75.0% of the bats were responsible for 99.8% of rectal shedding. Using a previously established approach (14, 57), two inoculated bats (452121 and 452049) were classified as supershedders for both oral and rectal RAVV shedding, as both shed at levels greater than the 80th percentile (oral = 4.18 $\log_{10}TCID_{50}$ equivalents/mL; rectal = 2.64 $\log_{10}TCID_{50}$ equivalents/mL, respectively) and together accounted for 69.4 and 89.2% of the total RAVV oral and rectal shedding, respectively. RAVV oral and rectal shedding was detected 12 and 10 times in bat 452121 and eight and six times in bat 452049, respectively. An infectious virus was isolated from four out of four (100%) oral swabs taken from bat 452121 and four out of five (80%) oral swabs taken from bat 452049.

No evidence of clinical disease

Consistent with previous MARV experimental studies in ERBs (14, 21), no disease-related morbidity or mortality was observed in any of the ERBs, and normal social and feeding behaviors were maintained. All bats maintained normal body weights and rectal temperatures, consistent with previous studies (Fig. 5) (21).
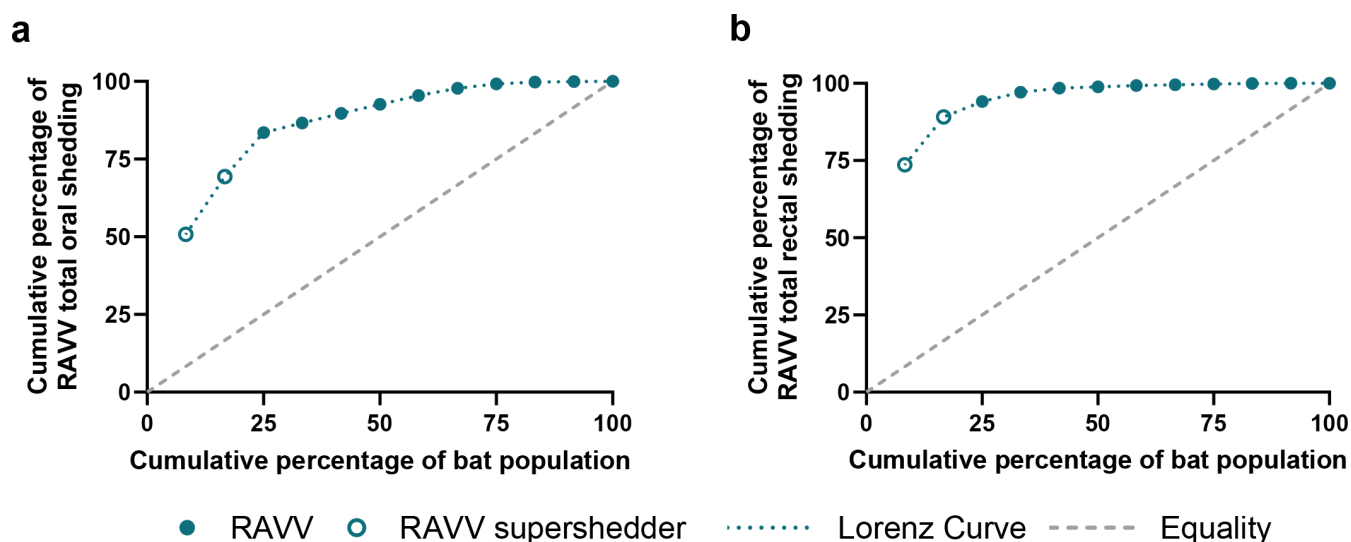

FIG 4 Cumulative RAVV shedding in experimentally infected Egyptian rousette bats. Lorenz curve of cumulative percentage of the inoculated bat population versus cumulative percentage of (a) oral and (b) rectal shedding ranked in descending order (i.e., the first circle on the circle represents bat 452121, which had the highest cumulative percentage of both rectal and oral shedding).
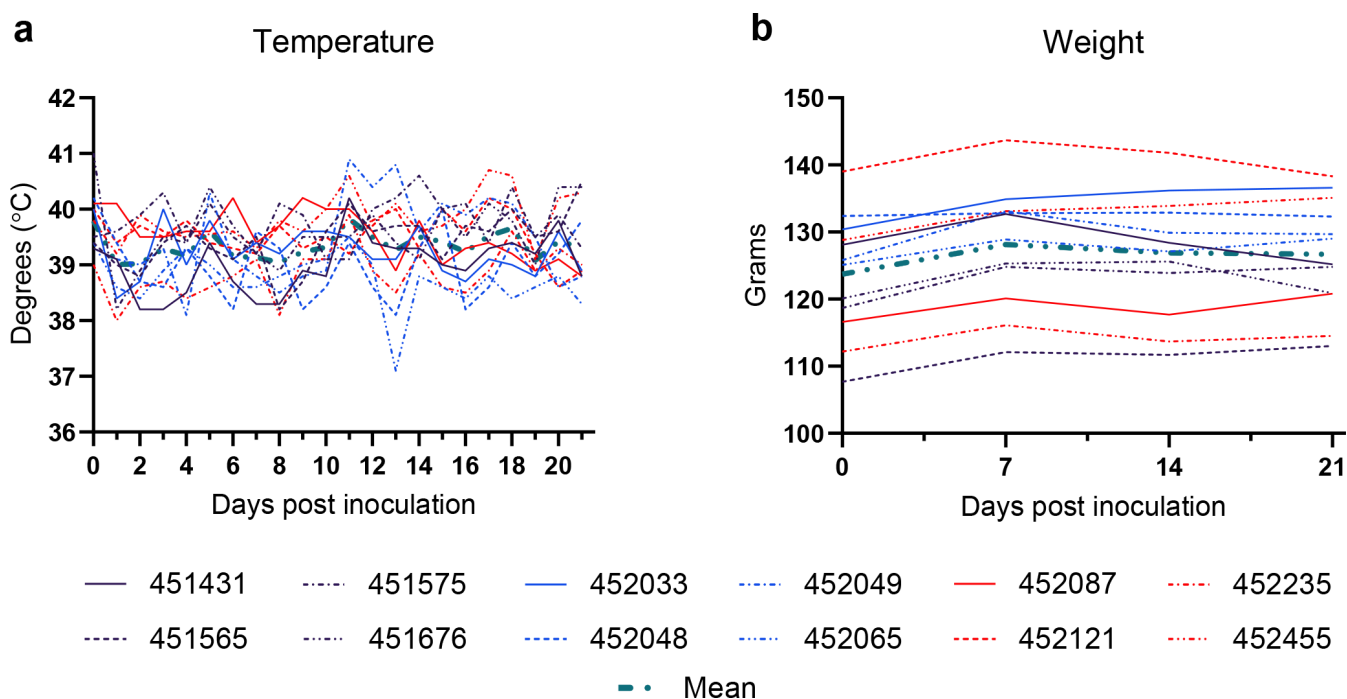
FIG 5 Clinical data. (a) Temperatures (°C) acquired via rectal thermometer and (b) weights (g) from experimentally infected Egyptian rousette bats.

DISCUSSION

This study provides the first measure of the shedding dynamics of experimental RAVV infection in ERBs, a natural reservoir host. Similar to MARV, RAVV reaches a viremic peak at approximately 5–6 DPI, with viral shedding peaking in oral secretions around 7 DPI and in fecal secretions around 6 DPI (14, 18, 21). These findings suggest that RAVV, like MARV, is likely horizontally transmitted through direct and/or indirect contact with infected bodily fluids (14, 21). A recent study found that infectious MARV can persist on contaminated fruit spats for up to 6 h, providing an additional route of exposure to other animals, including other bat species or other susceptible animal hosts, such as non-human primates (58).

A comparison between RAVV and MARV shedding dynamics can be drawn between the current study and that of Schuh et al. (14). In Schuh et al. (14), 12 naïve ERBs were subcutaneously inoculated with an identical experimental dose (four $\log_{10}TCID_{50}$) and route of MARV and underwent oral and rectal swab sampling over an identical timeline to the current RAVV study. While the infection timeline between MARV and RAVV is comparable, experimentally inoculated ERBs produce higher rectal RAVV shedding loads with a longer shedding duration compared to Schuh et al. (14), along with prolonged oral shedding and higher peak viremia (Fig. 3). This striking variation in rectal shedding may elucidate why, in a recent surveillance study of rectal swab samples from ERBs in South Africa, only RAVV was detected out of 416 samples tested (8).

It is currently unclear as to how these two orthomarburgviruses, RAVV and MARV, continue to circulate in free-ranging ERB populations yet remain genetically distinct. As mentioned earlier, the full genomic sequence of RAVV differs by up to 21% from MARV (Fig. 1), with the most notable variation (~22%) in the amino acid sequence of the RAVV glycoprotein (GP) (6, 16). Investigation into the generation of protective and cross-reactive monoclonal antibodies via exposure to engineered MARV GPs found that RAVV has four unique residues on the GP2 "wing," which is a 66-amino-acid N-terminal GP2 extension, when compared to other MARV variants (59). Additionally, a recent study investigating the use of mRNA vaccines against MARV and RAVV developed based on sequences of their respective GPs and glycan caps found differences in antibody

frequencies, antibody binding, neutralizing capacity, and linear epitope recognition (60). This suggests that the structural divergence between the GPs of distant orthomarburgviruses potentially affects stability, alterations, and/or the spatial location of domains (60). These differences may contribute to the differences noted between RAVV and MARV shedding in this study.

Variations in viral GPs of other viruses can have significant implications for infection and pathogenicity (61). For instance, a point mutation in the influenza C virus GP was found to increase receptor-binding efficiency (62). Similarly, mutations within the hepatitis C virus E2 GP increased its affinity to its receptor and reduced the virus' sensitivity to neutralization (63). An amino acid mutation in the GP of lymphocytic choriomeningitis virus (Clone 13 strain) is thought to be responsible for the long-term persistence of Clone 13 infections (64). Additionally, six mutations generated *in vitro* at the interface of Ebola virus (EBOV) GP_1 and GP_2 resulted in confirmational changes that rendered the virus independent of Cathepsin B, a protease required for EBOV cellular entry (65). Substitutions in many conserved residues of the MARV GP led to significant defects in GP expression, incorporation into HIV virions, and the ability to mediate viral entry (66). Furthermore, a naturally occurring polymorphism in the Sudan virus GP_1 decreased GP stability, therefore potentially affecting viral infectivity (67). These findings underscore the critical role of glycoprotein variations in viral infectivity, stability, and immune evasion, highlighting their potential as targets for therapeutic intervention and possibly explaining the variation in fecal shedding dynamics observed thus far in ERBs experimentally infected with either RAVV or MARV.

Variation in infection and shedding loads and their impact on disease transmission dynamics have been well documented in both human (49, 52, 68) and veterinary literature (14, 46, 48, 50, 57, 69–71) and linked to between- and within-host variations (53, 55, 69, 72), immune suppression (68), and viral (68, 73), bacterial (74–76), and/or parasitic co-infections (75). The Pareto Principle (or 80/20 rule) originally applied to wealth inequality states that ~80% of an effect (i.e., RAVV virus shedding) is produced by ~20% of the population (56, 57). This principle has been previously applied to experimental ERB MARV infection dynamics (14), where the Lorenz curve and the Gini coefficient are used to graphically represent and quantify the cumulative inequality in viral shedding to allow for identification of viral "supershedders" (57) within the experimental cohort. Super-spreaders, or supershedders, are individuals who infect or shed disproportionately more than most infected individuals and have been described in both natural (57, 69, 77) and experimental infections (14), in which the infectious exposure dose, time course, and inoculation route are standardized. In this study, we found that 25.0% of the bats were responsible for 83.5% of RAVV oral shedding, and 16.7% of the bats were responsible for 89.2% of the RAVV rectal shedding. Two bats (452121 and 452049) were classified as supershedders (57) for both oral and rectal RAVV shedding, as both shed at levels greater than the 80th percentile and accounted for 69.4 and 89.2% of the total RAVV oral and rectal shedding, respectively. Both supershedder bats also had prolonged shedding durations: bat 452121 shed RAVV orally for 12 days and rectally for 10 days, while bat 452049 shed RAVV orally for 8 days and rectally for 6 days. MARV loads detected in rectal swabs in Schuh et al. (14) were excluded from cumulative shedding calculations, making a direct comparison between MARV and RAVV cumulative rectal shedding unavailable. This heterogeneity in RAVV shedding loads and durations may contribute to the fitness of RAVV in natural outbred ERB populations. Additionally, the marked statistical significance in RAVV rectal shedding compared to MARV rectal shedding introduces the possibility that rectal shedding is a more robust component of environmental maintenance and spread for RAVV than it is for MARV.

Another factor that cannot be discounted in the variation in viral shedding dynamics between the current study and previous ERB MARV experimental studies could be age. Ecological studies have observed a seasonal pulse in viral circulation within natural bat reservoir hosts, with a higher prevalence of active infection in juvenile bats (~6 months old) (10, 78–80) and age-dependent variations in disease outcomes (81, 82).

This may reflect a "perfect storm" of reservoir infective permissiveness, in which the weaned juvenile bats are no longer protected by material antibodies, are susceptible to horizontal transmission of infectious disease within the densely packed roosts, and lack immunologic maturity to temper viral infection and subsequent shedding. As such, the standard experimental model for most MARV ERB research has been to use animals that are 5–7 months old to mimic the biological parameters found in free-ranging ERBs. Here, the ERBs in the current study were 12–14 months old, introducing the possibility that age-related variation in infection dynamics could be a factor in the observed experimental differences in viral rectal shedding.

This study shows that experimental RAVV infection in ERBs, a natural reservoir host for *Orthomarburgvirus marburgense* viruses, follows a similar viral shedding timeline as past experimental MARV infections in ERBs but with increased virus rectal shedding. Future work is needed to fully characterize the pathogenesis of experimental RAVV infection in ERBs, including evaluation of clinical, histochemical, and immunohistochemical findings and tissue viral loads at serial time points, with heightened focus on the small and large intestines. Future RAVV research could additionally include comparisons to Sosuga virus, a paramyxovirus for which the ERB serves as a putative natural reservoir, as Sosuga virus has been shown to replicate extensively in the small intestines (83). This work provides an important baseline for hypothesis-driven research, allowing a successful extrapolation of research findings in controlled laboratory settings to wild ERB populations and enabling experimental comparisons between MARV and RAVV infections.

MATERIALS AND METHODS

Animals and biosafety

All experimental procedures were conducted with approval from the Centers for Disease Control and Prevention (CDC, Atlanta, Georgia, USA) Institutional Animal Care and Use Committee and in strict accordance with the Guide for the Care and Use of Laboratory Animals (Committee for the Update of the Guide for the Care and Use of Laboratory Animals 2011). The CDC is a fully accredited research facility by the Association for Assessment and Accreditation of Laboratory Animal Care International. No recombinant or human patient-derived clinical materials were used in these studies.

Procedures conducted with infectious RAVV or infected bats were performed at the CDC under biosafety level 4 (BSL-4) laboratory conditions in accordance with select agent regulations (Animal and Plant Health Inspection Service and Centers for Disease Control and Prevention 2014). All investigators and animal handlers followed strict BSL-4 safety and infection control practices (84).

A total of 12 adult captive-born (21) ERBs (12–14 months old; six males and six females) were used in this study. The bats were housed in groups of six separated by sex in designated experimental and control caging (interior dimensions 61 × 71 × 76 cm long, wide, and high, respectively) in a climate-controlled BSL-4 laboratory animal room with a 12 h day/night cycle. The cages were housed within an isolation unit (Duo-Flow Mobile Units, Lab Products, Inc., Seaford, Delaware, USA) with high-efficiency particulate air-filtered inlet and exhaust air supply. The bats' daily food consisted of chopped bananas, watermelon, cantaloupe, seedless grapes, apples, and pears dusted with a protein vitamin supplement (Lubee Bat Conservancy, Gainesville, Florida, USA).

Virus

Following the experimental design of a previous MARV study (14), 4 $\log_{10}$ 50% tissue culture infective dose ($TCID_{50}$) of a RAVV isolate (188bat2007 virus; second passage on Vero E6 cells) obtained from a naturally infected ERB (188bat) collected during a 2007 orthomarburgvirus outbreak ecological investigation at Kitaka Mine in southwestern Uganda was prepared in 0.25 mL of sterile Dulbecco's modified Eagle's medium (6).

Experimental design

ERBs were acclimated in the BSL-4 laboratory for 7 days before the beginning of the study (acclimation phase). Baseline blood samples, body weights, and temperatures were recorded prior to inoculation. At 0 DPI, all 12 bats were inoculated subcutaneously under isoflurane anesthesia with the above-described RAVV inoculum in the caudal abdominal region. As data from historical MARV control ERBs from previous studies were available, control ERBs were not utilized in this study. Blood samples, oral swabs, rectal samples, and temperatures were recorded daily; body weight was measured on 0, 7, 14, and 21 DPI.

Specimen collection

Specimen collection has previously been described in detail (14, 18, 21). Blood (whole, nonheparinized; 10 and 21 µL for RT-qPCR and serology, respectively) was taken on −1 DPI and daily from 1 to 21 DPI from the cephalic wing vein using a sterile lancet (C&A Scientific, Manassas, VA, USA). Blood was tested for the presence of RAVV RNA by RT-qPCR through 15 DPI, and RAVV IgG antibody responses were monitored weekly through 21 DPI. The oral mucosa was sampled daily through 21 DPI by swabbing the inside of the bat's mouth and cheeks using two polyester-tipped applicators (Fisher Scientific, Grand Island, NY, USA). After sampling, one oral swab was immediately placed in either a deep-well plate with 500 µL of MagMAX lysis buffer solution (Life Technologies, Grand Island, New York, USA) for RT-qPCR analysis, and one oral swab was placed in sterile viral transport medium for attempted virus isolation of any RAVV RNA positive swabs. A temperature probe covered with a plastic sheath (MABIS Healthcare, Waukegan, Illinois, USA) was used to measure the daily rectal temperature of each bat. The plastic sheath was then cut and placed into a deep-well plate with 500 µL of MagMAX lysis buffer solution (Life Technologies) for fecal RT-qPCR analysis.

Euthanasia

At 22 DPI, all bats were euthanized under anesthesia via an overdose of isoflurane, followed by cardiac exsanguination. Cardiac blood was collected and retained.

Nucleic acid extraction

Nucleic acid was extracted from blood, oral swab, and rectal probe covers using the MagMAX Pathogen RNA/DNA Kit (Thermo Fisher Scientific, Waltham, MA, USA) on the MagMAX Express-96 Deep-well Magnetic Particle Processor (Thermo Fisher Scientific).

RT-qPCR

RT-qPCR procedures have been previously described in detail (14, 18, 21). Reverse-transcribed RAVV and ERB beta-2-microglobulin (B2M) RNA were detected on the CFX Opus 96 Real-time PCR System (Bio-Rad, Hercules, CA, USA) using the Luna Probe One-step RT-qPCR 4× Mix with UDG (New England Biolabs, Inc., Ipswich, MA, USA). The amplification utilized primers and reporter probes targeting the orthomarburgvirus viral protein 40 (VP40) gene (forward primer: GGACCACTGCTGGCCATATC, reverse primer: GAGAACATITCGGCAGGAAG, probe 1: 56-*FAM*-ATC CTA AAC-*ZEN*-AGG CTT GTC TTC TCT GGG ACT T-*3IABkFQ*, probe 2: 56-*FAM*-ATC CTG AAT-*ZEN*-AAG CTC GTC TTC TCT GGG ACT T-*3IABkFQ*) and the ERB B2M gene (forward primer: CAGCAAGGACTGGTCTTTCTAT, reverse primer: CCTCCATGATGCTGGTTAGTT, probe: *FAM*-TTC ACA CGG-*ZEN*-CAG CTG TAC TCA TCC-*3IABkFQ*), respectively. This assay was designed to detect a conserved sequence of VP40 present in all known species of orthomarburgvirus, including RAVV (16). Relative RAVV $TCID_{50}$eq/mL (blood and oral specimens) were interpolated from standard curves generated from serial dilutions of the titrated 188bat RAVV spiked into appropriate biological specimens. Based on testing triplicate 10-fold serial dilutions of RAVV ranging from 5.8×10^6 to $−1.12 \times 10^6$ $TCID_{50}$eq/mL, the lowest concentration of RAVV detected in all three replicates was 1.8×10^6 $TCID_{50}$eq/mL.

Virus isolation and immunofluorescence assay

Virus isolation and immunofluorescence assays have been previously described in detail (14, 18, 21). Virus isolation was attempted on RT-qPCR-positive oral swab samples for orthomarburgvirus with CT values ≤ 32. Initially, monolayers of 85% confluent Vero E6 cells (American Type Culture Collection, CRL-1586) in 25 cm^2 tissue culture flasks were inoculated with 100 µL viral transport medium from wells containing the positive oral swabs supplemented with 500 µL maintenance media (Dulbecco's Modified Eagle Medium containing 2%, heat-inactivated fetal bovine serum, 100 units/mL penicillin, 100 µg/mL streptomycin, and 2.50 µg/mL amphotericin B) and incubated for 1 h at 37°C/5% CO_2. Subsequently, 7 mL of maintenance media was added, and cultures were further incubated under the same conditions. At 7 and 14 DPI, tissue culture monolayers were scraped to release virus-infected cells. Next, 1.5 mL of each cellular medium was suspended in 8 mL borate saline. After centrifugation to pellet the cellular suspensions, borate saline was decanted, and the cells were resuspended in 500 µL borate saline. Then, 25 µL of the cellular resuspensions was spotted onto 12-well spot slides, which were fixed in acetone and exposed to 2 megarads of γ-irradiation.

All 7 and 14 DPI cultures were tested by immunofluorescence assay for orthomarburgvirus antigen. Spot slides were incubated with a 1:100 dilution of rabbit anti-MARV polyclonal (in-house) or normal rabbit serum (negative control; in-house) for 30 min at 37°C. Slides were then rinsed twice with 1× PBS for 10 min, followed by incubation with 1:40 dilution of goat anti-rabbit fluorescein isothiocyanate (Capel-ICN Pharmaceuticals, Aurora, OH, USA) for 30 min at 37°C. After a 7 min rinse with 1× PBS, the slides were stained with Eriochrome Black T (in-house) for 7 min, followed by another 7 min rinse with 1× PBS. The slides were then observed under a fluorescence microscope.

Serology

As previously described (14, 21, 22), ELISA plates were coated with 50 ng per well of purified recombinant Marburg Angola NP or Reston NP expressed in *Escherichia coli* (GenScript, Piscataway, NJ, USA) diluted in PBS containing 1% thimerosal. Following an overnight incubation at 4°C, the plates were washed with PBS containing 0.1% Tween-20 (PBS-T). A 1:100 dilution of gamma-irradiated bat whole blood in masterplate diluent (PBS containing 5% skim milk powder, 0.5% Tween-20, and 1% thimersol) was added to the first well, with subsequent fourfold serial dilutions in serum diluent (PBS containing 5% skim milk and 0.1% Tween-20) performed through 1:6,400. After incubating for 1 h at 37°C, the plates were washed with PBS-T, and bound antibodies were detected using a 1:11,000 dilution of anti-goat bat IgG (Bethyl Laboratories, Montgomery, TX, USA) in serum diluent. Following a 1 h incubation with the secondary antibody at 37°C, the plates were washed twice with PBS-T, and the 2-Component ABTS Peroxidase System (KPL, Gaithersburg, MD, USA) was added. The substrate was allowed to incubate for 30 min at 37°C before the plates were read on a microplate spectrophotometer at 410 nm.

To negate non-specific background reactivity, adjusted optical density (OD) values were calculated by subtracting the ODs at each fourfold dilution of wells coated with Reston NP from ODs at corresponding wells coated with MARV NP. The adjusted sum OD value was then linearly transformed using the min–max normalization method. The seropositivity threshold was set at 0.07 after in-house assay optimization.

Data and statistical analyses

Statistical analyses were completed as previously reported (14). Each comparator group comprised 12 bats. The number of bats per group was based on the reproductive capacity of the ERB breeding colony, the number of bats that could be safely handled daily, and the available space in the BSL-4 lab. Investigators were not blinded during the study, and no bats or individual data points were excluded from the analyses.

Excel (Microsoft 365, Redmond, WA) was used to manage data, and GraphPad Prism 10 (GraphPad, La Jolla, CA) was used to perform statistical analyses and generate figures.

The RAVV peak viral loads and the duration of viral shedding were determined for each bat according to the sample type (blood, oral swab, and rectal swab). To assess RAVV infectiousness, cumulative viral shedding loads were calculated for each bat by summing the viral loads detected in blood, oral swabs, and rectal swabs through the duration of the study. Using the approach of Jankowski et al. (57), bats were classified as supershedders if they shed RAVV at loads ≥ the 80th percentile. Raw data from Schuh et al. (14) were generously provided by the author for MARV statistical comparison.

The Shapiro–Wilk test was used to determine if the peak viral load, duration of viral shedding, and cumulative viral shedding load data sets followed a normal or lognormal distribution. If data sets were normally distributed, then unpaired t-tests were used to determine if parameter means differed significantly between RAVV and MARV bat groups. If data sets were lognormally distributed, they were log-transformed before using unpaired t-tests to determine if parameter geometric means differed significantly between RAVV and MARV bat groups. If data sets did not follow a normal or lognormal distribution, then non-parametric Mann–Whitney U tests were used to determine if the parameter mean ranks differed significantly between RAVV and MARV bat groups. All P values are two-tailed, and $P < 0.05$ is considered statistically significant. Each bat represents an individual biological replicate.

AUTHOR AFFILIATIONS

[1]Department of Pathology, College of Veterinary Medicine, University of Georgia, Athens, Georgia, USA

[2]Viral Special Pathogens Branch, Division of High-Consequence Pathogens and Pathology, National Center for Emerging and Zoonotic Infectious Diseases, United States Centers for Disease Control and Prevention, Atlanta, Georgia, USA

[3]USA Public Health Service Commissioned Corps, Rockville, Maryland, USA

AUTHOR ORCIDs

Jessica A. Elbert http://orcid.org/0000-0001-7862-0830
Amy J. Schuh http://orcid.org/0000-0001-8069-349X
Jonathan S. Towner http://orcid.org/0000-0002-6473-3049

AUTHOR CONTRIBUTIONS

Jessica A. Elbert, Conceptualization, Formal analysis, Investigation, Methodology, Visualization, Writing – original draft, Writing – review and editing.

DATA AVAILABILITY

All data generated or analyzed during this study are included in this published article or are available upon request from the corresponding author.

REFERENCES

1. Brauburger K, Hume AJ, Mühlberger E, Olejnik J. 2012. Forty-five years of Marburg virus research. Viruses 4:1878–1927. https://doi.org/10.3390/v4101878

2. Siegert R, Shu HL, Slenczka HL, Peters D, Müller G. 1968. The aetiology of an unknown human infection transmitted by monkeys (preliminary communication). Ger Med Mon 13:1–2.

3. Venkatesan P. 2025. Marburg virus outbreak in Tanzania. Lancet Microbe:101121. https://doi.org/10.1016/j.lanmic.2025.101121

4. Johnson ED, Johnson BK, Silverstein D, Tukei P, Geisbert TW, Sanchez AN, Jahrling PB. 1996. Characterization of a new Marburg virus isolated from a 1987 fatal case in Kenya. Arch Virol Suppl 11:101–114. https://doi.org/10.1007/978-3-7091-7482-1_10

5. Bausch DG, Nichol ST, Muyembe-Tamfum JJ, Borchert M, Rollin PE, Sleurs H, Campbell P, Tshioko FK, Roth C, Colebunders R, et al. 2006. Marburg hemorrhagic fever associated with multiple genetic lineages of virus. N Engl J Med 355:909–919. https://doi.org/10.1056/NEJMoa051465

6. Towner JS, Amman BR, Sealy TK, Carroll SAR, Comer JA, Kemp A, Swanepoel R, Paddock CD, Balinandi S, Khristova ML, et al. 2009. Isolation of genetically diverse Marburg viruses from Egyptian fruit bats. PLoS Pathog 5:e1000536. https://doi.org/10.1371/journal.ppat.1000536

7. Pigott DM, Golding N, Mylne A, Huang Z, Weiss DJ, Brady OJ, Kraemer MUG, Hay SI. 2015. Mapping the zoonotic niche of Marburg virus disease in Africa. Trans R Soc Trop Med Hyg 109:366–378. https://doi.org/10.1093/trstmh/trv024

8. Pawęska JT, Storm N, Markotter W, Di Paola N, Wiley MR, Palacios G, Jansen van Vuren P. 2020. Shedding of Marburg virus in naturally infected Egyptian rousette bats, South Africa, 2017. Emerg Infect Dis 26:3051–3055. https://doi.org/10.3201/eid2612.202108

9. Kwiecinski GG, Griffiths TA. 1999. *Rousettus egyptiacus*. Mammalian Species 611:1. https://doi.org/10.2307/3504411

10. Amman BR, Carroll SA, Reed ZD, Sealy TK, Balinandi S, Swanepoel R, Kemp A, Erickson BR, Comer JA, Campbell S, et al. 2012. Seasonal pulses of Marburg virus circulation in juvenile *Rousettus aegyptiacus* bats coincide with periods of increased risk of human infection. PLoS Pathog 8:e1002877. https://doi.org/10.1371/journal.ppat.1002877

11. Jones MEB, Amman BR, Sealy TK, Ueblehoer LS, Schuh AJ, Flietstra T, Bird BH, Coleman-McCray JD, Zaki SR, Nichol ST, Towner JS. 2019. Clinical, histopathologic, and immunohistochemical characterization of experimental Marburg virus infection in a natural reservoir host, the Egyptian rousette bat (*Rousettus aegyptiacus*). Viruses 11:214. https://doi.org/10.3390/v11030214

12. Pawęska JT, Jansen van Vuren P, Kemp A, Storm N, Grobbelaar AA, Wiley MR, Palacios G, Markotter W. 2018. Marburg virus infection in Egyptian rousette bats, South Africa, 2013–2014. Emerg Infect Dis 24:1134–1137. https://doi.org/10.3201/eid2406.172165

13. Swanepoel R, Smit SB, Rollin PE, Formenty P, Leman PA, Kemp A, Burt FJ, Grobbelaar AA, Croft J, Bausch DG, Zeller H, Leirs H, Braack LEO, Libande ML, Zaki S, Nichol ST, Ksiazek TG, Paweska JT, International Scientific and Technical Committee for Marburg Hemorrhagic Fever Control in the Democratic Republic of Congo. 2007. Studies of reservoir hosts for Marburg virus. Emerg Infect Dis 13:1847–1851. https://doi.org/10.3201/eid1312.071115

14. Schuh AJ, Amman BR, Jones MEB, Sealy TK, Uebelhoer LS, Spengler JR, Martin BE, Coleman-McCray JAD, Nichol ST, Towner JS. 2017. Modelling filovirus maintenance in nature by experimental transmission of Marburg virus between Egyptian rousette bats. Nat Commun 8:14446. https://doi.org/10.1038/ncomms14446

15. Amman BR, Nyakarahuka L, McElroy AK, Dodd KA, Sealy TK, Schuh AJ, Shoemaker TR, Balinandi S, Atimnedi P, Kaboyo W, Nichol ST, Towner JS. 2014. Marburgvirus resurgence in Kitaka Mine bat population after extermination attempts, Uganda. Emerg Infect Dis 20:1761–1764. https://doi.org/10.3201/eid2010.140696

16. Towner JS, Khristova ML, Sealy TK, Vincent MJ, Erickson BR, Bawiec DA, Hartman AL, Comer JA, Zaki SR, Ströher U, Gomes da Silva F, del Castillo F, Rollin PE, Ksiazek TG, Nichol ST. 2006. Marburgvirus genomics and association with a large hemorrhagic fever outbreak in Angola. J Virol 80:6497–6516. https://doi.org/10.1128/JVI.00069-06

17. Carroll SA, Towner JS, Sealy TK, McMullan LK, Khristova ML, Burt FJ, Swanepoel R, Rollin PE, Nichol ST. 2013. Molecular evolution of viruses of the family Filoviridae based on 97 whole-genome sequences. J Virol 87:2608–2616. https://doi.org/10.1128/JVI.03118-12

18. Jones MEB, Schuh AJ, Amman BR, Sealy TK, Zaki SR, Nichol ST, Towner JS. 2015. Experimental inoculation of Egyptian rousette bats (*Rousettus aegyptiacus*) with viruses of the Ebolavirus and Marburgvirus genera. Viruses 7:3420–3442. https://doi.org/10.3390/v7072779

19. Paweska JT, Jansen van Vuren P, Fenton KA, Graves K, Grobbelaar AA, Moolla N, Leman P, Weyer J, Storm N, McCulloch SD, Scott TP, Markotter W, Odendaal L, Clift SJ, Geisbert TW, Hale MJ, Kemp A. 2015. Lack of Marburg virus transmission from experimentally infected to susceptible in-contact Egyptian fruit bats. J Infect Dis 212 Suppl 2:S109–18. https://doi.org/10.1093/infdis/jiv132

20. Paweska JT, Jansen van Vuren P, Masumu J, Leman PA, Grobbelaar AA, Birkhead M, Clift S, Swanepoel R, Kemp A. 2012. Virological and serological findings in *Rousettus aegyptiacus* experimentally inoculated with vero cells-adapted hogan strain of Marburg virus. PLoS One 7:e45479. https://doi.org/10.1371/journal.pone.0045479

21. Amman BR, Jones MEB, Sealy TK, Uebelhoer LS, Schuh AJ, Bird BH, Coleman-McCray JD, Martin BE, Nichol ST, Towner JS. 2015. Oral shedding of Marburg virus in experimentally infected Egyptian fruit bats (*Rousettus aegyptiacus*). J Wildl Dis 51:113–124. https://doi.org/10.7589/2014-08-198

22. Schuh AJ, Amman BR, Sealy TK, Spengler JR, Nichol ST, Towner JS. 2017. Egyptian rousette bats maintain long-term protective immunity against Marburg virus infection despite diminished antibody levels. Sci Rep 7:8763. https://doi.org/10.1038/s41598-017-07824-2

23. Guito JC, Kirejczyk SGM, Schuh AJ, Amman BR, Sealy TK, Graziano J, Spengler JR, Harmon JR, Wozniak DM, Prescott JB, Towner JS. 2024. Coordinated inflammatory responses dictate Marburg virus control by reservoir bats. Nat Commun 15:1826. https://doi.org/10.1038/s41467-024-46226-7

24. Arnold CE, Guito JC, Altamura LA, Lovett SP, Nagle ER, Palacios GF, Sanchez-Lockhart M, Towner JS. 2018. Transcriptomics reveal antiviral gene induction in the Egyptian rousette bat is antagonized *in vitro* by marburg virus infection. Viruses 10:607. https://doi.org/10.3390/v10110607

25. Nakayama E, Saijo M. 2013. Animal models for Ebola and Marburg virus infections. Front Microbiol 4:267. https://doi.org/10.3389/fmicb.2013.00267

26. Glaze ER, Roy MJ, Dalrymple LW, Lanning LL. 2015. A comparison of the pathogenesis of Marburg virus disease in humans and nonhuman Primates and evaluation of the suitability of these animal models for predicting clinical efficacy under the 'Animal Rule'. Comp Med 65:241–259.

27. Cross RW, Fenton KA, Geisbert JB, Ebihara H, Mire CE, Geisbert TW. 2015. Comparison of the pathogenesis of the Angola and Ravn strains of Marburg virus in the outbred guinea pig model. J Infect Dis 212 Suppl 2:S258–70. https://doi.org/10.1093/infdis/jiv182

28. Geisbert TW, Strong JE, Feldmann H. 2015. Considerations in the use of nonhuman primate models of Ebola virus and Marburg virus infection. J Infect Dis 212 Suppl 2:S91–S97. https://doi.org/10.1093/infdis/jiv284

29. Warfield KL, Bradfute SB, Wells J, Lofts L, Cooper MT, Alves DA, Reed DK, VanTongeren SA, Mech CA, Bavari S. 2009. Development and characterization of a mouse model for Marburg hemorrhagic fever. J Virol 83:6404–6415. https://doi.org/10.1128/JVI.00126-09

30. Krähling V, Dolnik O, Kolesnikova L, Schmidt-Chanasit J, Jordan I, Sandig V, Günther S, Becker S. 2010. Establishment of fruit bat cells (*Rousettus aegyptiacus*) as a model system for the investigation of filoviral infection. PLoS Negl Trop Dis 4:e802. https://doi.org/10.1371/journal.pntd.0000802

31. Larson PA, Bartlett ML, Garcia K, Chitty J, Balkema-Buschmann A, Towner J, Kugelman J, Palacios G, Sanchez-Lockhart M. 2021. Genomic features of humoral immunity support tolerance model in Egyptian rousette bats. Cell Rep 35:109140. https://doi.org/10.1016/j.celrep.2021.109140

32. Shifflett K, Marzi A. 2019. Marburg virus pathogenesis - differences and similarities in humans and animal models. Virol J 16:165. https://doi.org/10.1186/s12985-019-1272-z

33. Cooper TK, Sword J, Johnson JC, Bonilla A, Hart R, Liu DX, Bernbaum JG, Cooper K, Jahrling PB, Hensley LE. 2018. New insights into Marburg virus disease pathogenesis in the rhesus macaque model. J Infect Dis 218:S423–S433. https://doi.org/10.1093/infdis/jiy367

34. Bradfute SB, Warfield KL, Bray M. 2012. Mouse models for filovirus infections. Viruses 4:1477–1508. https://doi.org/10.3390/v4091477

35. Gentles AD, Guth S, Rozins C, Brook CE. 2020. A review of mechanistic models of viral dynamics in bat reservoirs for zoonotic disease. Pathog Glob Health 114:407–425. https://doi.org/10.1080/20477724.2020.1833161

36. Reynolds P, Marzi A. 2017. Ebola and Marburg virus vaccines. Virus Genes 53:501–515. https://doi.org/10.1007/s11262-017-1455-x

37. Cross RW, Mire CE, Feldmann H, Geisbert TW. 2018. Post-exposure treatments for Ebola and Marburg virus infections. Nat Rev Drug Discov 17:413–434. https://doi.org/10.1038/nrd.2017.251

38. Grant-Klein RJ, Van Deusen NM, Badger CV, Hannaman D, Dupuy LC, Schmaljohn CS. 2012. A multiagent filovirus DNA vaccine delivered by intramuscular electroporation completely protects mice from ebola and Marburg virus challenge. Hum Vaccin Immunother 8:1703–1706. https://doi.org/10.4161/hv.21873

39. Wang D, Hevey M, Juompan LY, Trubey CM, Raja NU, Deitz SB, Woraratanadharm J, Luo M, Yu H, Swain BM, Moore KM, Dong JY. 2006. Complex adenovirus-vectored vaccine protects guinea pigs from three strains of Marburg virus challenges. Virology (Auckl) 353:324–332. https://doi.org/10.1016/j.virol.2006.05.033

40. Mire CE, Geisbert JB, Borisevich V, Fenton KA, Agans KN, Flyak AI, Deer DJ, Steinkellner H, Bohorov O, Bohorova N, Goodman C, Hiatt A, Kim DH, Pauly MH, Velasco J, Whaley KJ, Crowe JE Jr, Zeitlin L, Geisbert TW. 2017. Therapeutic treatment of Marburg and Ravn virus infection in nonhuman primates with a human monoclonal antibody. Sci Transl Med 9:eaai8711. https://doi.org/10.1126/scitranslmed.aai8711

41. Thi EP, Mire CE, Lee AC, Geisbert JB, Ursic-Bedoya R, Agans KN, Robbins M, Deer DJ, Cross RW, Kondratowicz AS, Fenton KA, MacLachlan I, Geisbert TW. 2017. siRNA rescues nonhuman primates from advanced Marburg and Ravn virus disease. J Clin Invest 127:4437–4448. https://doi.org/10.1172/JCI96185

42. Wong G, Zhang Z, He S, de La Vega M-A, Tierney K, Soule G, Tran K, Fernando L, Qiu X. 2018. Marburg and Ravn virus infections do not cause observable disease in ferrets. J Infect Dis 218:S471–S474. https://doi.org/10.1093/infdis/jiy245

43. Cross RW, Mire CE, Agans KN, Borisevich V, Fenton KA, Geisbert TW. 2018. Marburg and Ravn viruses fail to cause disease in the domestic ferret (Mustela putorius furo). J Infect Dis 218:S448–S452. https://doi.org/10.1093/infdis/jiy268

44. Nicholas VV, Rosenke R, Feldmann F, Long D, Thomas T, Scott DP, Feldmann H, Marzi A. 2018. Distinct biological phenotypes of Marburg and Ravn virus infection in macaques. J Infect Dis 218:S458–S465. https://doi.org/10.1093/infdis/jiy456

45. Storm N, Jansen Van Vuren P, Markotter W, Paweska JT. 2018. Antibody responses to Marburg virus in Egyptian rousette bats and their role in protection against infection. Viruses 10:73. https://doi.org/10.3390/v10020073

46. Courcoul A, Monod H, Nielen M, Klinkenberg D, Hogerwerf L, Beaudeau F, Vergu E. 2011. Modelling the effect of heterogeneity of shedding on the within herd Coxiella burnetii spread and identification of key parameters by sensitivity analysis. J Theor Biol 284:130–141. https://doi.org/10.1016/j.jtbi.2011.06.017

47. Fleming-Davies AE, Dukic V, Andreasen V, Dwyer G. 2015. Effects of host heterogeneity on pathogen diversity and evolution. Ecol Lett 18:1252–1261. https://doi.org/10.1111/ele.12506

48. Lambert S, Gilot-Fromont E, Freycon P, Thébault A, Game Y, Toïgo C, Petit E, Barthe M-N, Reynaud G, Jaÿ M, Garin-Bastuji B, Ponsart C, Hars J, Rossi S. 2018. High shedding potential and significant individual heterogeneity in naturally-infected Alpine ibex (Capra ibex) with Brucella melitensis. Front Microbiol 9:1065. https://doi.org/10.3389/fmicb.2018.01065

49. Lau LLH, Ip DKM, Nishiura H, Fang VJ, Chan K-H, Peiris JSM, Leung GM, Cowling BJ. 2013. Heterogeneity in viral shedding among individuals with medically attended influenza A virus infection. J Infect Dis 207:1281–1285. https://doi.org/10.1093/infdis/jit034

50. Matthews L, Low JC, Gally DL, Pearce MC, Mellor DJ, Heesterbeek JAP, Chase-Topping M, Naylor SW, Shaw DJ, Reid SWJ, Gunn GJ, Woolhouse MEJ. 2006. Heterogeneous shedding of Escherichia coli O157 in cattle and its implications for control. Proc Natl Acad Sci U S A 103:547–552. https://doi.org/10.1073/pnas.0503776103

51. Matthews L, Reeve R, Woolhouse MEJ, Chase-Topping M, Mellor DJ, Pearce MC, Allison LJ, Gunn GJ, Low JC, Reid SWJ. 2009. Exploiting strain diversity to expose transmission heterogeneities and predict the impact of targeting supershedding. Epidemics 1:221–229. https://doi.org/10.1016/j.epidem.2009.10.002

52. Milbrath MO, Spicknall IH, Zelner JL, Moe CL, Eisenberg JNS. 2013. Heterogeneity in norovirus shedding duration affects community risk. Epidemiol Infect 141:1572–1584. https://doi.org/10.1017/S0950268813000496

53. Siva-Jothy JA, Vale PF. 2021. Dissecting genetic and sex-specific sources of host heterogeneity in pathogen shedding and spread. PLoS Pathog 17:e1009196. https://doi.org/10.1371/journal.ppat.1009196

54. VanderWaal KL, Ezenwa VO. 2016. Heterogeneity in pathogen transmission. Func Ecol 30:1606–1622. https://doi.org/10.1111/1365-2435.12645

55. White LA, Forester JD, Craft ME. 2018. Covariation between the physiological and behavioral components of pathogen transmission: host heterogeneity determines epidemic outcomes. Oikos 127:538–552. https://doi.org/10.1111/oik.04527

56. Woolhouse ME, Dye C, Etard JF, Smith T, Charlwood JD, Garnett GP, Hagan P, Hii JL, Ndhlovu PD, Quinnell RJ, Watts CH, Chandiwana SK, Anderson RM. 1997. Heterogeneities in the transmission of infectious agents: implications for the design of control programs. Proc Natl Acad Sci U S A 94:338–342. https://doi.org/10.1073/pnas.94.1.338

57. Jankowski MD, Williams CJ, Fair JM, Owen JC. 2013. Birds shed RNA-viruses according to the pareto principle. PLoS One 8:e72611. https://doi.org/10.1371/journal.pone.0072611

58. Amman BR, Schuh AJ, Albariño CG, Towner JS. 2021. Marburg virus persistence on fruit as a plausible route of bat to primate filovirus transmission. Viruses 13:2394. https://doi.org/10.3390/v13122394

59. Fusco ML, Hashiguchi T, Cassan R, Biggins JE, Murin CD, Warfield KL, Li S, Holtsberg FW, Shulenin S, Vu H, Olinger GG, Kim DH, Whaley KJ, Zeitlin L, Ward AB, Nykiforuk C, Aman MJ, Berry JD, Saphire EO. 2015. Protective mAbs and cross-reactive mAbs raised by immunization with engineered Marburg virus GPs. PLoS Pathog 11:e1005016. https://doi.org/10.1371/journal.ppat.1005016

60. Bukreyev A, Meyer M, Gunn B, Pietzsch C, Subramani C, Saphire E, Crowe J, Alter G, Himansu S, Carfi A. 2024. Divergent antibody recognition profiles are generated by protective mRNA vaccines against Marburg and Ravn viruses. In Review. https://doi.org/10.21203/rs.3.rs-4087897/v1

61. Yang ZY, Duckers HJ, Sullivan NJ, Sanchez A, Nabel EG, Nabel GJ. 2000. Identification of the Ebola virus glycoprotein as the main viral determinant of vascular cell cytotoxicity and injury. Nat Med 6:886–889. https://doi.org/10.1038/78645

62. Szepanski S, Gross HJ, Brossmer R, Klenk HD, Herrler G. 1992. A single point mutation of the influenza C virus glycoprotein (HEF) changes the viral receptor-binding activity. Virology (Auckl) 188:85–92. https://doi.org/10.1016/0042-6822(92)90737-a

63. Dhillon S, Witteveldt J, Gatherer D, Owsianka AM, Zeisel MB, Zahid MN, Rychłowska M, Foung SKH, Baumert TF, Angus AGN, Patel AH. 2010. Mutations within a conserved region of the hepatitis C virus E2 glycoprotein that influence virus-receptor interactions and sensitivity to neutralizing antibodies. J Virol 84:5494–5507. https://doi.org/10.1128/JVI.02153-09

64. Sullivan BM, Emonet SF, Welch MJ, Lee AM, Campbell KP, de la Torre JC, Oldstone MB. 2011. Point mutation in the glycoprotein of lymphocytic choriomeningitis virus is necessary for receptor binding, dendritic cell infection, and long-term persistence. Proc Natl Acad Sci U S A 108:2969–2974. https://doi.org/10.1073/pnas.1019304108

65. Wong AC, Sandesara RG, Mulherkar N, Whelan SP, Chandran K. 2010. A forward genetic strategy reveals destabilizing mutations in the Ebolavirus glycoprotein that alter its protease dependence during cell entry. J Virol 84:163–175. https://doi.org/10.1128/JVI.01832-09

66. Manicassamy B, Wang J, Rumschlag E, Tymen S, Volchkova V, Volchkov V, Rong L. 2007. Characterization of Marburg virus glycoprotein in viral entry. Virology (Auckl) 358:79–88. https://doi.org/10.1016/j.virol.2006.06.041

67. Lennemann NJ, Dillard J, Ruggio N, Cooney AL, Schaack GA, Davey RA, Maury W. 2021. A naturally occurring polymorphism in the base of Sudan virus glycoprotein decreases glycoprotein stability in a species-dependent manner. J Virol 95:e0107321. https://doi.org/10.1128/JVI.01073-21

68. Witteck A, Yerly S, Vernazza P. 2009. Unusually high HIV infectiousness in an HIV-, HCV- and HSV-2-coinfected heterosexual man. Swiss Med Wkly 139:207–209. https://doi.org/10.4414/smw.2009.12575

69. Chase-Topping M, Gally D, Low C, Matthews L, Woolhouse M. 2008. Super-shedding and the link between human infection and livestock carriage of Escherichia coli O157. Nat Rev Microbiol 6:904–912. https://doi.org/10.1038/nrmicro2029

70. Cobbold RN, Hancock DD, Rice DH, Berg J, Stilborn R, Hovde CJ, Besser TE. 2007. Rectoanal junction colonization of feedlot cattle by *Escherichia coli* O157:H7 and its association with supershedders and excretion dynamics. Appl Environ Microbiol 73:1563–1568. https://doi.org/10.1128/AEM.01742-06

71. Nowak K, Fahr J, Weber N, Lübke-Becker A, Semmler T, Weiss S, Mombouli J-V, Wieler LH, Guenther S, Leendertz FH, Ewers C. 2017. Highly diverse and antimicrobial susceptible *Escherichia coli* display a naïve bacterial population in fruit bats from the Republic of Congo. PLoS ONE 12:e0178146. https://doi.org/10.1371/journal.pone.0178146

72. Barfield M, Orive ME, Holt RD. 2015. The role of pathogen shedding in linking within-and between-host pathogen dynamics. Math Biosci 270:249–262. https://doi.org/10.1016/j.mbs.2015.04.010

73. Augenbraun M, Feldman J, Chirgwin K, Zenilman J, Clarke L, DeHovitz J, Landesman S, Minkoff H. 1995. Increased genital shedding of herpes simplex virus type 2 in HIV-seropositive women. Ann Intern Med 123:845–847. https://doi.org/10.7326/0003-4819-123-11-199512010-00006

74. Cohen MS, Hoffman IF, Royce RA, Kazembe P, Dyer JR, Daly CC, Zimba D, Vernazza PL, Maida M, Fiscus SA, Eron JJ Jr. 1997. Reduction of concentration of HIV-1 in semen after treatment of urethritis: implications for prevention of sexual transmission of HIV-1. AIDSCAP Malawi Research Group. Lancet 349:1868–1873. https://doi.org/10.1016/s0140-6736(97)02190-9

75. Lass S, Hudson PJ, Thakar J, Saric J, Harvill E, Albert R, Perkins SE. 2013. Generating super-shedders: co-infection increases bacterial load and egg production of a gastrointestinal helminth. J R Soc Interface 10:20120588. https://doi.org/10.1098/rsif.2012.0588

76. Stein RA, Bianchini EC. 2022. Bacterial-viral interactions: a factor that facilitates transmission heterogeneities. FEMS Microbes 3:xtac018. https://doi.org/10.1093/femsmc/xtac018

77. Lukicheva N, Ebel ED, Williams MS, Schlosser WD. 2016. Characterizing the concentration of pathogen occurrence across meat and poultry industries. Microbial Risk Analysis 4:29–35. https://doi.org/10.1016/j.mran.2016.05.002

78. Wacharapluesadee S, Duengkae P, Chaiyes A, Kaewpom T, Rodpan A, Yingsakmongkon S, Petcharat S, Phengsakul P, Maneeorn P, Hemachudha T. 2018. Longitudinal study of age-specific pattern of coronavirus infection in Lyle's flying fox (*Pteropus lylei*) in Thailand. Virol J 15:38. https://doi.org/10.1186/s12985-018-0950-6

79. Rahman SA, Hassan L, Epstein JH, Mamat ZC, Yatim AM, Hassan SS, Field HE, Hughes T, Westrum J, Naim MS, Suri AS, Jamaluddin AA, Daszak P, Henipavirus Ecology Research Group. 2013. Risk factors for Nipah virus infection among pteropid bats, Peninsular Malaysia. Emerg Infect Dis 19:51–60. https://doi.org/10.3201/eid1901.120221

80. Peel AJ, Baker KS, Hayman DTS, Broder CC, Cunningham AA, Fooks AR, Garnier R, Wood JLN, Restif O. 2018. Support for viral persistence in bats from age-specific serology and models of maternal immunity. Sci Rep 8:3859. https://doi.org/10.1038/s41598-018-22236-6

81. Brändel SD, Tschapka M, Page R, Rasche A, Corman VM, Drosten C, Sommer S. 2018. Astrovirus infections induce age-dependent dysbiosis in gut microbiomes of bats. ISME J 12:2883–2893. https://doi.org/10.1038/s41396-018-0239-1

82. Mendenhall IH, Skiles MM, Neves ES, Borthwick SA, Low DHW, Liang B, Lee BPY-H, Su YCF, Smith GJD. 2017. Influence of age and body condition on astrovirus infection of bats in Singapore: an evolutionary and epidemiological analysis. One Health 4:27–33. https://doi.org/10.1016/j.onehlt.2017.10.001

83. Kirejczyk SGM, Amman BR, Schuh AJ, Sealy TK, Albariño CG, Zhang J, Brown CC, Towner JS. 2022. Histopathologic and immunohistochemical evaluation of induced lesions, tissue tropism and host responses following experimental infection of Egyptian rousette bats (*Rousettus aegyptiacus*) with the zoonotic paramyxovirus, Sosuga virus. Viruses 14:1278. https://doi.org/10.3390/v14061278

84. Meechan PJ, Potts J, Ed. 2020. Biosafety in microbiological and biomedical laboratories. In Centers for Disease Control and Prevention, National Institutes of Health, 6th ed. https://stacks.cdc.gov/view/cdc/97733.